HHS Public Access

Author manuscript

Nature. Author manuscript; available in PMC 2018 May 01.

Published in final edited form as:

Nature. 2012 December 20; 492(7429): 428–432. doi:10.1038/nature11617.

A prefrontal cortex–brainstem neuronal projection that controls response to behavioural challenge

Melissa R. Warden[1,9], **Aslihan Selimbeyoglu**[1,2], **Julie J. Mirzabekov**[1], **Maisie Lo**[3], **Kimberly R. Thompson**[1], **Sung-Yon Kim**[1,2], **Avishek Adhikari**[1], **Kay M. Tye**[1,6], **Loren M. Frank**[7,8], and **Karl Deisseroth**[1,2,4,5,9]

[1]Department of Bioengineering, Stanford, CA, U.S.A

[2]Neurosciences Program, Stanford, CA, U.S.A

[3]Bio-X Program, Stanford, CA, U.S.A

[4]Department of Psychiatry and Behavioral Sciences, Stanford, CA, U.S.A

[5]Howard Hughes Medical Institute Stanford University, Stanford, CA, U.S.A

[6]Picower Institute for Learning and Memory, Department of Brain and Cognitive Sciences Massachusetts Institute of Technology, Cambridge, MA, U.S.A

[7]Department of Physiology, San Francisco, San Francisco, CA, U.S.A

[8]W.M. Keck Center for Integrative Neuroscience University of California, San Francisco, San Francisco, CA, U.S.A

Abstract

The prefrontal cortex (PFC) is thought to participate in high-level control over generation of behaviors (including the decision to execute actions[1]); indeed, imaging and lesion studies in human beings have revealed that PFC dysfunction can lead to either impulsive states with increased tendency to initiate action[2], or to amotivational states characterized by hopeless and depressive symptoms[3]. In light of the opposite valence of these two phenotypes as well as the broad complexity of other tasks attributed to PFC, it may be that only a specific subclass of PFC neurons favors effortful behavioral responses to challenging situations. Here we develop and employ a quantitative method for continuous assessment and control of active response to behavioral challenge, synchronized with single-unit electrophysiology and optogenetics in freely moving rats. We first observed by recording in the medial PFC (mPFC) that many neurons were

[9]To whom correspondence should be addressed: deissero@stanford.edu, mwarden@stanford.edu.

Author Contributions

M.R.W., L.M.F., and K.D. contributed to study design with assistance from A.S. and K.M.T. M.R.W., L.M.F., and K.D. contributed to data interpretation and manuscript revision. M.R.W., A.S., K.M.T., J.M., M.L., K.R.T., S-Y.K., and A.A. contributed to data collection. M.R.W. coordinated all experiments, developed the induction coil and forced swim test electrophysiology methods, and performed all behavioral and *in vivo* electrophysiology analyses. K.D. supervised all aspects of the project. M.R.W and K.D. wrote the paper.

Readers are welcome to comment on the online version of this article at www.nature.com/nature. M.R.W. and K.D. have disclosed these findings to the Stanford Office of Technology Licensing, which has filed a patent application for possible use in identifying new treatments for depression. All materials, methods, and reagents remain freely available for academic and nonprofit research in perpetuity via www.optogenetics.org.

not simply movement-related in their spike firing patterns, but instead were selectively modulated from moment to moment according to the animal's decision to act in a challenging situation. Surprisingly, we next found that direct activation of principal neurons in the mPFC had no detectable causal effect on this behavior. We next tested if this behavior could be causally mediated by only a subclass of mPFC cells defined by specific downstream wiring. Indeed, by leveraging optogenetic projection-targeting to control cells with specific efferent wiring patterns, we observed that selective activation of those mPFC cells projecting to the brainstem dorsal raphe nucleus (DRN), a serotonergic nucleus implicated in major depressive disorder[4], induced a profound, rapid, and reversible effect on selection of the active behavioral state. These results may be of importance in understanding the circuit basis of normal and pathological patterns of action selection and motivation in behavior.

Acting to expend energy with vigorous effort under challenging conditions represents a consequential decision for an organism, especially since such action may not always represent the most adaptive behavior. When a vigorous action pattern is selected despite extremely difficult circumstances (rather than a more energy-conserving passive or depressive-type pattern), an assessment may have occurred that anticipated outcomes justify expenditure of energy. Conversely, when an organism selects inactive behavioral patterns in challenging situations, the decision may represent anticipation that effort is likely to be fruitless. Such anticipation leading to inaction can become maladaptive in human beings, with clinical symptoms including psychomotor retardation and hopelessness (core defining features of major depression, a disease with lifetime prevalence of nearly 20% and extensive socioeconomic ramifications[5]).

We sought to probe these high-level processes governing behavioral state selection with targeted control of restricted sets of circuit elements in freely moving mammals. Mounting evidence suggests that the prefrontal cortex (PFC) could be involved in these behaviors; the PFC is responsible for coordinating thought and action, and has been shown to be critical for goal-oriented behavior, planning, and cognitive control[6,7] – all of which are impaired in pathological states such as depression[8–11]. Moreover, deep brain stimulation of the subcallosal cingulate region of the PFC elicits antidepressant effects in treatment-resistant patients[12]. Electrical stimulation of the rodent mPFC induces an antidepressant-like reduction in immobility in the forced swim test[13], optogenetic stimulation of mixed excitatory and inhibitory neural populations in mPFC has an antidepressant-like effect in social defeat[14], and mPFC in rodents appears to mediate resilience[15]. Finally, neuroimaging studies in human patients have been instrumental in focusing attention on brain regions including PFC that exhibit abnormal activity in depression and melancholic states[3,16,17].

Despite these pioneering efforts pointing to the PFC, it is unclear which specific neural pathways are involved in real-time selection of effortful behavioral responses to challenging situations. The forced swim test (FST) is relevant to this issue, as a widely-employed behavioral test in rodents[18]. In the FST, rodents are placed in an inescapable tank of water and epochs of passive floating, which are thought to reflect states of behavioral despair[18], are interspersed with epochs of active escape behavior; immobility in the FST is influenced by antidepressant drugs[19] and stress[20]. Transitions between active escape and behavioral

despair states in the FST are clearly demarcated, in principle providing an unambiguous, instantaneous classification of a specific motivated behavioral state and an opportunity to investigate the neural dynamics underlying the decision to adopt an active behavioral response to challenge. However, to our knowledge, neural activity has never been recorded in behaving animals during the FST because of the fundamental technical obstacles of recording and controlling neural activity in a freely swimming animal. To address this challenge we developed a new set of methods for recording millisecond-precision neural and behavioral data alongside optogenetic control during the FST (Fig. 1).

We designed a magnetic induction method to detect individual swim kicks, in which the FST tank of water was surrounded by an induction coil and a small magnet was attached to the hind paw (Fig. 1a). During the FST each kick induced a current in the coil (Fig. 1b); it was possible to cleanly isolate single kicks (Supplementary Fig. 1), and kick frequency and automatically scored immobility corresponded well to manually scored immobility (Fig. 1c,d). We additionally employed this method to record mobile and immobile states during cage activity (Supplementary Fig. 2). In order to record well-isolated single units during swimming, tetrode microdrives or fixed wire arrays were waterproofed (Supplementary Methods). Under these conditions we were reliably able to isolate single units during the FST (Fig. 1e); indeed, we were able to detect transitions between active escape behavior and immobile states with high temporal precision and to correlate these behaviors with ongoing neural activity (Fig. 2).

We recorded neural activity using either a 4-tetrode microdrive (6 rats) or a 24-electrode fixed-wire array (5 rats) targeted to the mPFC (Fig. 2a). Three epochs of data were recorded (Fig. 2b): a 15 minute pre-FST epoch in a familiar cage, 15 minutes during the FST, and 15 minutes post-FST. We found that many mPFC neurons were strongly modulated during behavior in a way that appeared to specifically reflect the decision to act or refrain from action during the FST. An example neuron is shown (Fig. 2c-d). This neuron was highly active during the mostly-immobile pre- and post-FST epochs (98% and 94% immobile, respectively), but during the FST it stayed active during mobile states and was inhibited during immobile states. This neuron did not simply encode locomotor activity, but was instead specifically inhibited during FST immobility corresponding to traditionally defined states of behavioral despair[18].

We found many neurons in the recorded population (23/160, 14%; see Supplementary Methods) exhibiting this surprising profile of activity. All rats exhibited minimal motor activity during the pre-FST epoch (greater than 88% immobility for all rats, average 97% immobility) and a moderate to high level of motor activity during the FST epoch (less than 79% immobility for all rats, average 39% immobility, Fig. 2e). Most recorded neurons (129/160, 81%) showed a significant change in firing rate between pre-FST and FST epochs (Fig. 2f, top). On average, this population of neurons was inhibited during the FST epoch (80/129, 62%). Many neurons (70/160, 44%) also showed a difference in firing rate between mobile and immobile states within the FST epoch (Fig. 2f, bottom). Most of these neurons were activated during mobile states and inhibited during immobile states (51/70, 73%).

We then examined the joint distribution of epoch- and mobility-dependent neural selectivity among four quadrants (Fig. 2g), and found it to be highly asymmetric. The upper right and lower left quadrants exhibited a straightforward correspondence between motor activity and neural activity; for example, neurons in the upper right quadrant were more active during the largely mobile FST epoch than during the immobile pre-FST epoch, and, within the FST epoch, were more active during mobile states. The other two quadrants (the upper left and lower right quadrants) showed an inverted correspondence. In the upper left quadrant, neurons that were quieted during the more-active FST epoch were actually activated during escape behaviors within FST, and the neurons in the lower right quadrant did the opposite. The profile of activity found within these groups was therefore not simply dependent on motor activity. We noted that putative fast-spiking interneurons (Supplementary Methods) exhibited a reduced degree of modulation along both selectivity dimensions. Finally, we found that when mPFC neural activity was aligned to the onset of mobility epochs, firing on average preceded the onset of mobility (Supplementary Fig. 3).

Because the mPFC neurons that we recorded exhibited a range of selectivity profiles, it was not obvious that optogenetically activating local neurons in the mPFC would have a net effect on behavior during the FST. To test this, we restricted opsin expression to CaMKIIα-expressing (chiefly excitatory) neurons within the mPFC using an adeno-associated viral vector (AAV5) expressing channelrhodopsin-2 fused to enhanced yellow fluorescent protein (ChR2-EYFP) under the control of the CaMKIIα promoter. Virus was infused into the mPFC and fiber optics were implanted over the mPFC (Fig. 3a-b). We confirmed functional targeting of these neurons with anesthetized optrode recordings in the mPFC (Supplementary Fig. 4a), but surprisingly, when these neurons were illuminated in two-minute epochs during the FST (Supplementary Methods), we found that stimulation was not sufficient to cause even a slight reduction in FST immobility (Fig. 3c, Wilcoxon signed-rank test, $p=0.23$) or change in a control open-field-test behavior (OFT, Supplementary Fig. 4b). One interpretation of these results is that local mPFC neurons may correlate with, but are not causally involved in, the behavioral state changes associated with effort-related mobility and immobility; alternatively, it could be that some local mPFC neurons are so involved, but others are not or are opposed in causal function, and when driven together no net effect on behavior is seen. We therefore next hypothesized that it could be possible to induce a change in this motivated behavioral state by restricting optogenetic stimulation to a reduced population of mPFC neurons.

The mPFC is known to project to several downstream brain regions that have been implicated in motivated behavior and depression[21]; among these is the dorsal raphe nucleus (DRN)[22], a serotonergic nucleus implicated in major depressive disorder[4]. The mPFC exerts control over both neural activity in the DRN and extracellular 5-HT levels[15,23], and antidepressant-like effects of mPFC electrical stimulation appear to depend on an intact 5-HT system[13], but the projection from the mPFC to the DRN has not been directly shown to have an effect on behavior. In order to specifically activate the mPFC-DRN projection, we first transduced excitatory neurons in the mPFC with AAV5 CaMKIIα::ChR2-EYFP (Fig. 3d), which led to robust ChR2-EYFP expression in mPFC axons in the DRN (Fig. 3e; Supplementary Fig. 5a). We restricted activation to the subpopulation of excitatory neurons in the mPFC that project to the DRN by implanting a fiber optic over the DRN and

selectively illuminating the mPFC axons in this region (Fig. 3d). We confirmed functional targeting with anesthetized optrode recordings (Supplementary Fig. 5b).

When the axons of ChR2-EYFP-expressing mPFC neurons in the DRN were stimulated during the FST, a profound change in effortful behavior resulted. Example induction-coil behavioral traces from two rats are shown (one ChR2-EYFP and one EYFP rat, Fig. 3f-g), demonstrating a robust increase in kick frequency during each light epoch in the ChR2-EYFP case. This behavioral effect was present in most ChR2-EYFP rats (Wilcoxon signed-rank test, p=1.04e-11) but not EYFP rats (Wilcoxon signed-rank test, p=0.39), and was rapid, reversible, and repeatable (Fig. 3h-i). Importantly, stimulation of this projection did not affect nonspecific locomotor activity in the open field in either ChR2-EYFP rats (Wilcoxon signed-rank test, p=0.59) or EYFP rats (Wilcoxon signed-rank test, p=0.71, Fig. 3j). This result demonstrates the importance of resolving subpopulations defined by projection target, and illustrates a causal role of a specific mPFC-to-brainstem neural pathway in driving this motivated behavioral response to a challenging environment. Additional experiments addressing the effect of mPFC-DRN stimulation on mPFC neural activity are described in Supplementary Figs. 6-9.

The mPFC projection to the DRN sends sparse collaterals to other brain regions[24]; we accordingly next blocked incoming glutamatergic synaptic activity in the DRN during stimulation of DRN-projecting mPFC axons (Supplementary Fig. 10). Glutamate receptor antagonists blocked stimulation-driven behavioral activation, revealing that activation of the mPFC-DRN synapse itself is necessary for the stimulation-induced increase in mobility. Additionally, inhibition of mPFC axons in the DRN led to a lasting decrease in steady-state mobility in the FST (Supplementary Fig. 11), pointing to the necessity of this pathway in normal behavior.

Hypothesizing that the specificity of the effect of mPFC on DRN would not be fully captured by general activation of the downstream region, we next directly tested this question by transducing neurons in the DRN with ChR2-EYFP under the control of the human synapsin-1 promoter (AAV5 hSyn::ChR2-EYFP), which transduced both 5-HT and GABA neurons in the DRN (Supplementary Fig. 12), and implanted a fiber optic directly above DRN (Fig. 4a-c). When ChR2-EYFP-expressing DRN cell bodies were directly illuminated, rats exhibited behavioral activation during the FST (Wilcoxon signed-rank test, p=5.63e-8), while EYFP-expressing rats did not (Wilcoxon signed-rank test, p=0.84, Fig. 4d,e). However, direct activation of the DRN, unlike stimulation of the mPFC-DRN projection, led to a general increase in locomotor activity in the OFT in ChR2-EYFP rats (Wilcoxon signed-rank test, p=0.02) but not EYFP rats (Wilcoxon signed-rank test, p=0.31, Fig. 4f). It is likely that mPFC-DRN stimulation and direct DRN cell body stimulation activate different sub-networks within the DRN, which may explain these dissimilar behavioral results.

Finally, we targeted the projection from the mPFC to the lateral habenula (LHb)[25], a region known to play an important role in motivated behavior and depression[26,27], and found that activation of this specific projection actually had the opposite effect on escape-related behavior in the FST. As above, we infused AAV5 CaMKIIα::ChR2-EYFP into the mPFC

and implanted bilateral fiber optics over the LHb (Fig. 4g-i). When ChR2-EYFP-expressing LHb-projecting mPFC axons were illuminated during the FST rats showed a rapid and reversible decrease in mobility (Wilcoxon signed-rank test, p=3.63e-4), while control EYFP-expressing rats did not (Wilcoxon signed-rank test, p=0.29, Fig. 4j-l, Supplementary Fig. 13).

Here, we have probed both neural correlates and causal neural pathways involved in the selection of an effortful motivated behavioral pattern during challenging circumstances, using novel technology permitting electrical recordings and optogenetic control in the FST in combination with high-speed readout of behavioral state. We have demonstrated the existence of different physiologically-defined mPFC neural populations– one selectively inhibited during behavioral despair-like states, and the other selectively activated. We have also demonstrated that, while general activation of CaMKIIα-expressing neurons in the mPFC does not have a net effect on this behavior in rats, selective activation in DRN or LHb of projecting mPFC neurons elicits distinct, rapid and reversible effects on selection of the active behavioral state. These results describe the neural dynamics associated with the behavioral response to challenge and demonstrate the causal importance of mPFC control of downstream targets in implementing this response, with implications for understanding both normal and pathological states of decision refinement and behavioral pattern selection.

Methods Summary

Male Long-Evans rats were implanted with either a 4-tetrode microdrive or a 24-electrode fixed wire array targeted to the mPFC. Tetrodes were adjusted daily. Prior to the start of recordings rats were anesthetized for 10 minutes to facilitate waterproofing of the headstage and electrodes and were subsequently allowed to recover for at least 1 hour. Data were analyzed in Matlab and Neuroexplorer with custom-written software.

The pAAV-CaMKIIα::hChR2(H134R)-eYFP, pAAV-CaMKIIα::eYFP, pAAV-CaMKIIα::eNpHR3.0-eYFP, and pAAV-hSyn::hChR2(H134R)-eYFP plasmids were designed and constructed by standard methods and packaged as AAV_5. Virus was injected into the mPFC or the DRN. Maps and clones are available at optogenetics.org.

The mPFC was virally transduced and an optical fiber was surgically implanted in separate surgeries over the DRN or the LHb to allow for selective illumination of mPFC axons. Cannulae were used instead for pharmacology experiments. Virus was allowed to express for a minimum of 4 months after injection for projection-targeting experiments. Behavioral data were collected 7-10 days after fiber implantation.

To confirm opsin expression, coronal brain slices were prepared for immunohistochemistry and optical microscopy. Brain sections were stained for DAPI and either rabbit anti-5-HT or rabbit anti-GABA. Sections were imaged with a confocal microscope.

Supplementary Material

Refer to Web version on PubMed Central for supplementary material.

Acknowledgments

We would like to thank H. Mayberg, R. Malenka, L. Gunaydin, J. Mattis, I. Ellwood, and I. Witten for helpful comments on the manuscript, I. Ellwood, I. Witten, R. Airan, L. Meltzer, M. Roy, V. Gradinaru, A. Andalman, T. Davidson, R. Durand, M. Bower, and M. Carr for useful discussions, and the entire K.D. laboratory for their support. We are grateful to S. Pak, C. Ramakrishnan, and C. Perry for technical assistance. Supported by the Wiegers Family Fund (K.D.), NARSAD (M.R.W. and K.R.T.), Stanford Graduate Fellowship (A.S.), Samsung Scholarship (S.-Y.K.), Berry Foundation Fellowship (A.A.), NIMH (1F32MH088010-01, K.M.T.), and NIMH, NIDA, the DARPA REPAIR Program, the Keck Foundation, the McKnight Foundation, the Yu, Snyder, Tarlton, and Woo Foundations, and the Gatsby Charitable Foundation (K.D.).

References

1. McGuire JT, Botvinick MM. Prefrontal cortex, cognitive control, and the registration of decision costs. Proceedings of the National Academy of Sciences of the United States of America. 2010; 107:7922–6. [PubMed: 20385798]
2. Ridderinkhof KR, van den Wildenberg WPM, Segalowitz SJ, Carter CS. Neurocognitive mechanisms of cognitive control: the role of prefrontal cortex in action selection, response inhibition, performance monitoring, and reward-based learning. Brain and cognition. 2004; 56:129–40. [PubMed: 15518930]
3. Mayberg HS, et al. Reciprocal limbic-cortical function and negative mood: converging PET findings in depression and normal sadness. The American journal of psychiatry. 1999; 156:675–82. [PubMed: 10327898]
4. Maes M, Meltzer H. The serotonin hypothesis of major depression. Psychopharmacology: the fourth generation of progress. 1995:933–44.
5. Kessler RC, et al. Lifetime prevalence and age-of-onset distributions of mental disorders in the World Health Organization's World Mental Health Survey Initiative. World psychiatry: official journal of the World Psychiatric Association (WPA). 2007; 6:168–76. [PubMed: 18188442]
6. Miller EK, Cohen JD. An integrative theory of prefrontal cortex function. Annual review of neuroscience. 2001; 24:167–202.
7. Fuster, JM. The Prefrontal Cortex, Fourth Edition. Academic Press; Waltham, Massachusetts: 2008.
8. Elliott R, et al. Prefrontal dysfunction in depressed patients performing a complex planning task: a study using positron emission tomography. Psychological medicine. 1997; 27:931–42. [PubMed: 9234470]
9. Austin MP. Cognitive deficits in depression: Possible implications for functional neuropathology. The British Journal of Psychiatry. 2001; 178:200–206. [PubMed: 11230029]
10. Ingram RE, Bernet CZ, McLaughlin SC. Attentional allocation processes in individuals at risk for depression. Cognitive Therapy and Research. 1994; 18:317–332.
11. Dalgleish T, Watts FN. Biases of attention and memory in disorders of anxiety and depression. Clinical Psychology Review. 1990; 10:589–604.
12. Mayberg HS, et al. Deep brain stimulation for treatment-resistant depression. Neuron. 2005; 45:651–60. [PubMed: 15748841]
13. Hamani C, et al. Antidepressant-like effects of medial prefrontal cortex deep brain stimulation in rats. Biological psychiatry. 2010; 67:117–24. [PubMed: 19819426]
14. Covington HE, et al. Antidepressant effect of optogenetic stimulation of the medial prefrontal cortex. The Journal of Neuroscience. 2010; 30:16082–90. [PubMed: 21123555]
15. Amat J, et al. Medial prefrontal cortex determines how stressor controllability affects behavior and dorsal raphe nucleus. Nature neuroscience. 2005; 8:365–71. [PubMed: 15696163]
16. Drevets WC. Neuroimaging and neuropathological studies of depression: implications for the cognitive-emotional features of mood disorders. Current opinion in neurobiology. 2001; 11:240–9. [PubMed: 11301246]
17. Baxter LR, et al. Reduction of prefrontal cortex glucose metabolism common to three types of depression. Archives of general psychiatry. 1989; 46:243–50. [PubMed: 2784046]
18. Porsolt R, Le Pichon M, Jalfre M. Depression: a new animal model sensitive to antidepressant treatments. Nature. 1977; 266:730–732. [PubMed: 559941]

19. Cryan JF, Valentino RJ, Lucki I. Assessing substrates underlying the behavioral effects of antidepressants using the modified rat forced swimming test. Neuroscience and biobehavioral reviews. 2005; 29:547–69. [PubMed: 15893822]
20. Willner P. Chronic mild stress (CMS) revisited: consistency and behavioural-neurobiological concordance in the effects of CMS. Neuropsychobiology. 2005; 52:90–110. [PubMed: 16037678]
21. Vertes RP. Differential projections of the infralimbic and prelimbic cortex in the rat. Synapse. 2004; 51:32–58. [PubMed: 14579424]
22. Gonçalves L, Nogueira MI, Shammah-Lagnado SJ, Metzger M. Prefrontal afferents to the dorsal raphe nucleus in the rat. Brain research bulletin. 2009; 78:240–7. [PubMed: 19103268]
23. Celada P, Puig MV, Casanovas JM, Guillazo G, Artigas F. Control of dorsal raphe serotonergic neurons by the medial prefrontal cortex: Involvement of serotonin-1A, GABA(A), and glutamate receptors. The Journal of Neuroscience. 2001; 21:9917–29. [PubMed: 11739599]
24. Gabbott PLA, Warner TA, Jays PRL, Salway P, Busby SJ. Prefrontal cortex in the rat: projections to subcortical autonomic, motor, and limbic centers. The Journal of comparative neurology. 2005; 492:145–77. [PubMed: 16196030]
25. Kim U, Lee T. Topography of descending projections from anterior insular and medial prefrontal regions to the lateral habenula of the epithalamus in the rat. The European journal of neuroscience. 2012; 35:1253–69. [PubMed: 22512256]
26. Matsumoto M, Hikosaka O. Representation of negative motivational value in the primate lateral habenula. Nature neuroscience. 2009; 12:77–84. [PubMed: 19043410]
27. Sartorius A, et al. Remission of major depression under deep brain stimulation of the lateral habenula in a therapy-refractory patient. Biological psychiatry. 2010; 67:e9–e11. [PubMed: 19846068]

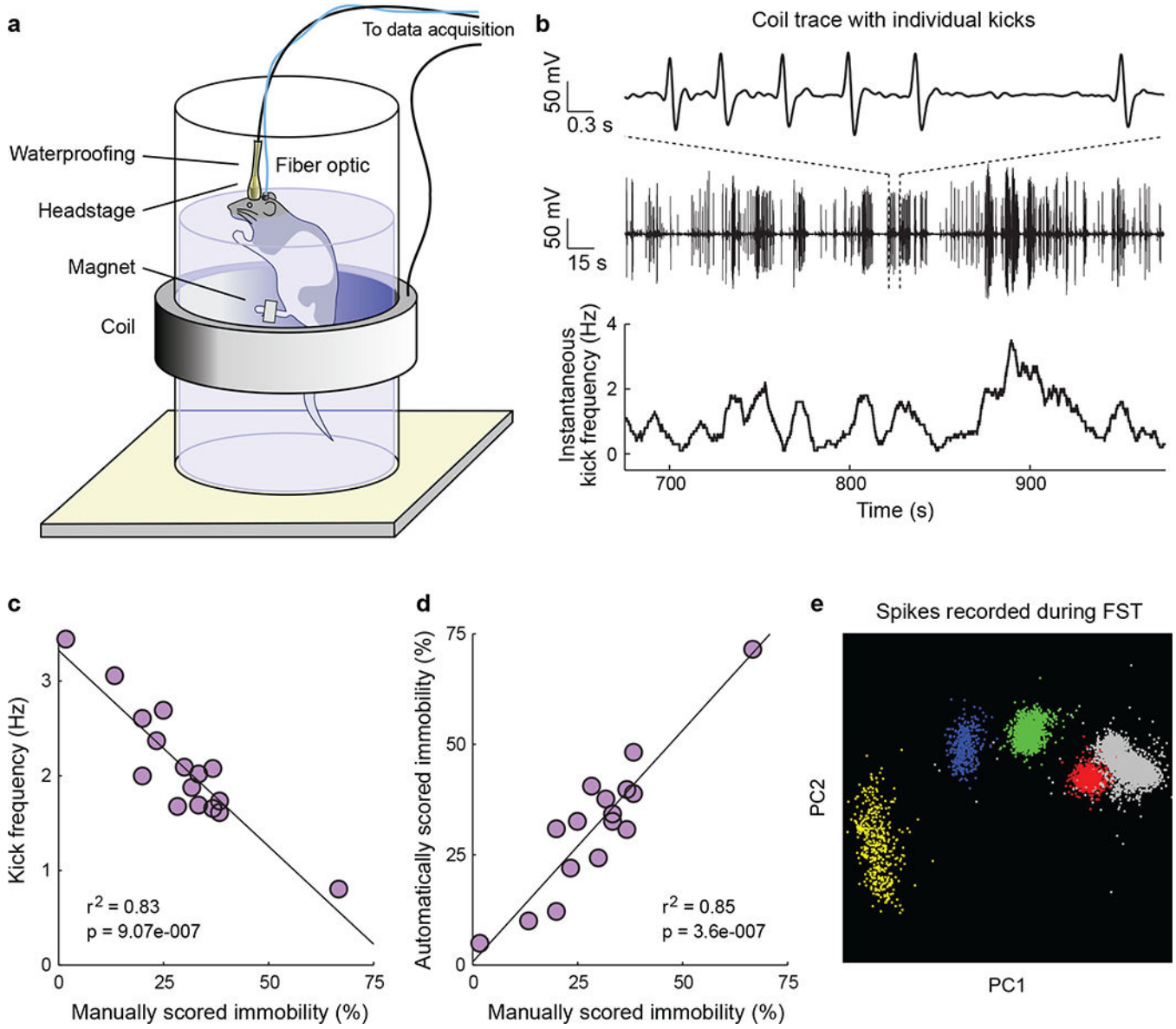

Figure 1. The automated FST provides a high temporal resolution behavioral readout that can be synchronized with simultaneously recorded neural data

a) A schematic of the automated FST. A coil of wire surrounds the tank of water and a magnet is attached to the rat's back paw. Movement of the magnet within the coil during swimming induces a current that can be recorded. To permit concurrent neural recordings the headstage is waterproofed. An optical fiber can be included for simultaneous optical stimulation. **b)** Example FST coil voltage traces. Top: a 6-second coil trace showing individual kicks. Middle: a 5-minute coil trace. Bottom: Instantaneous kick frequency estimated from the 5-minute coil trace. **c)** Average kick frequency corresponds well to manually scored immobility estimates. **d)** Estimates of FST immobility derived from the induction coil correspond tightly to manually scored immobility estimates. **e)** 4 well-isolated single mPFC units recorded during the FST.

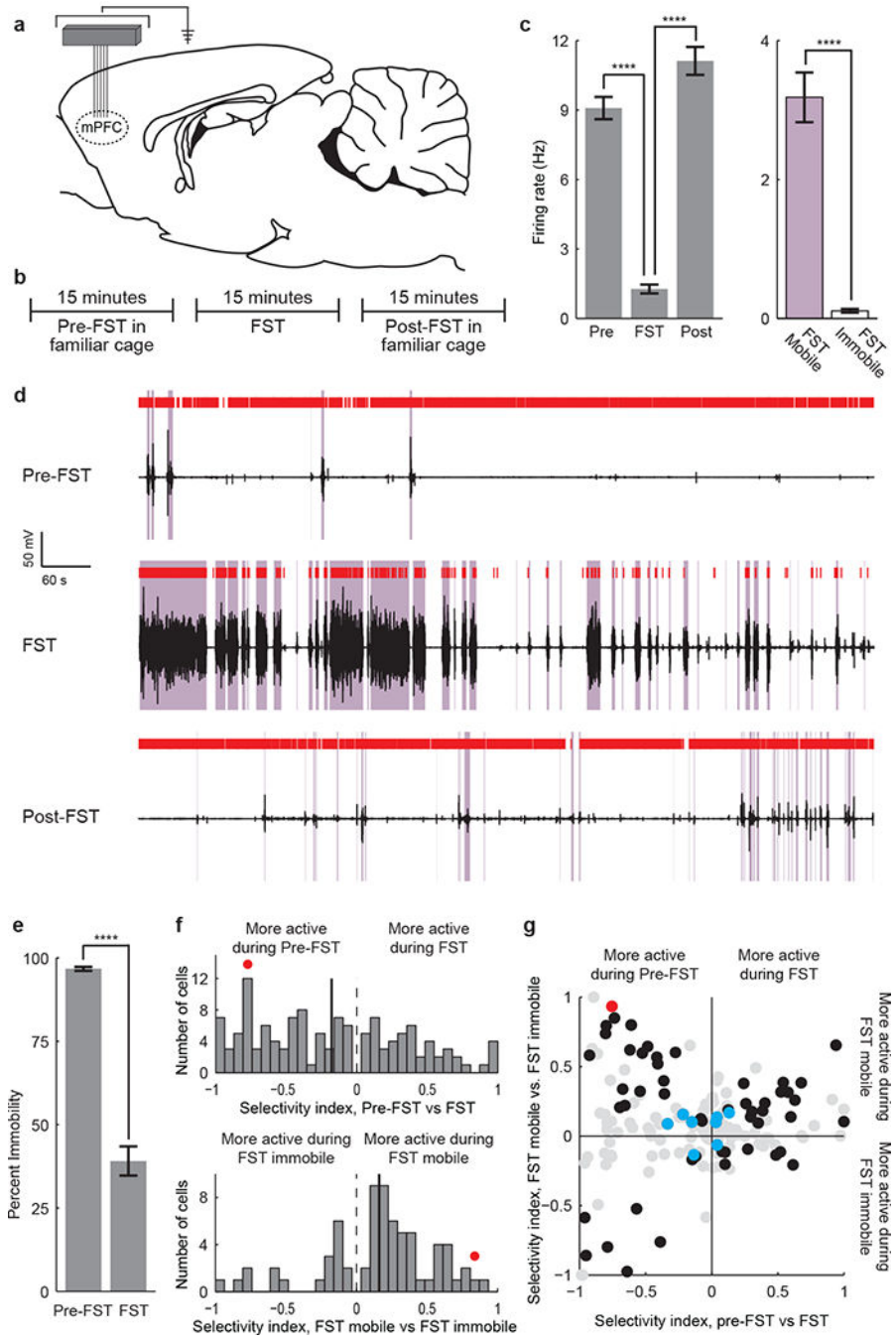

Figure 2. Prefrontal neuronal activity encodes FST behavioral state

a) A tetrode microdrive or fixed wire array was implanted over the mPFC. **b)** 15 minutes of data were recorded pre-FST, 15 minutes during the FST, and 15 minutes post-FST. **c)** Bar plot of an example neuron that is inhibited during immobile states in the FST. (Mann-Whitney U test, * $p<0.05$; ** $p<0.01$; *** $p<0.001$; **** $p<0.0001$). **d)** Raster plot of the same neuron. Coil voltage in black, mobile states in purple, spikes in red. Top: pre-FST activity. Middle: activity during the FST. Bottom: post-FST activity. **e)** Immobility during the pre-FST and FST test epochs (11 rats). **f)** Distribution of population selectivity indices

(Supplementary Methods). Top: pre-FST vs. FST epochs. All neurons significantly selective for pre-FST vs. FST are shown. Bottom: mobile vs. immobile FST states. All neurons significantly selective for mobile vs. immobile FST state are shown. **g)** Joint distribution of selectivity indices. Black circles: neurons selective for both task epoch and mobility. Red circle: example neuron. Blue circles: putative inhibitory fast-spiking neurons. Gray circles: non-significantly selective neurons. All recorded neurons are shown. Error bars indicate s.e.m.

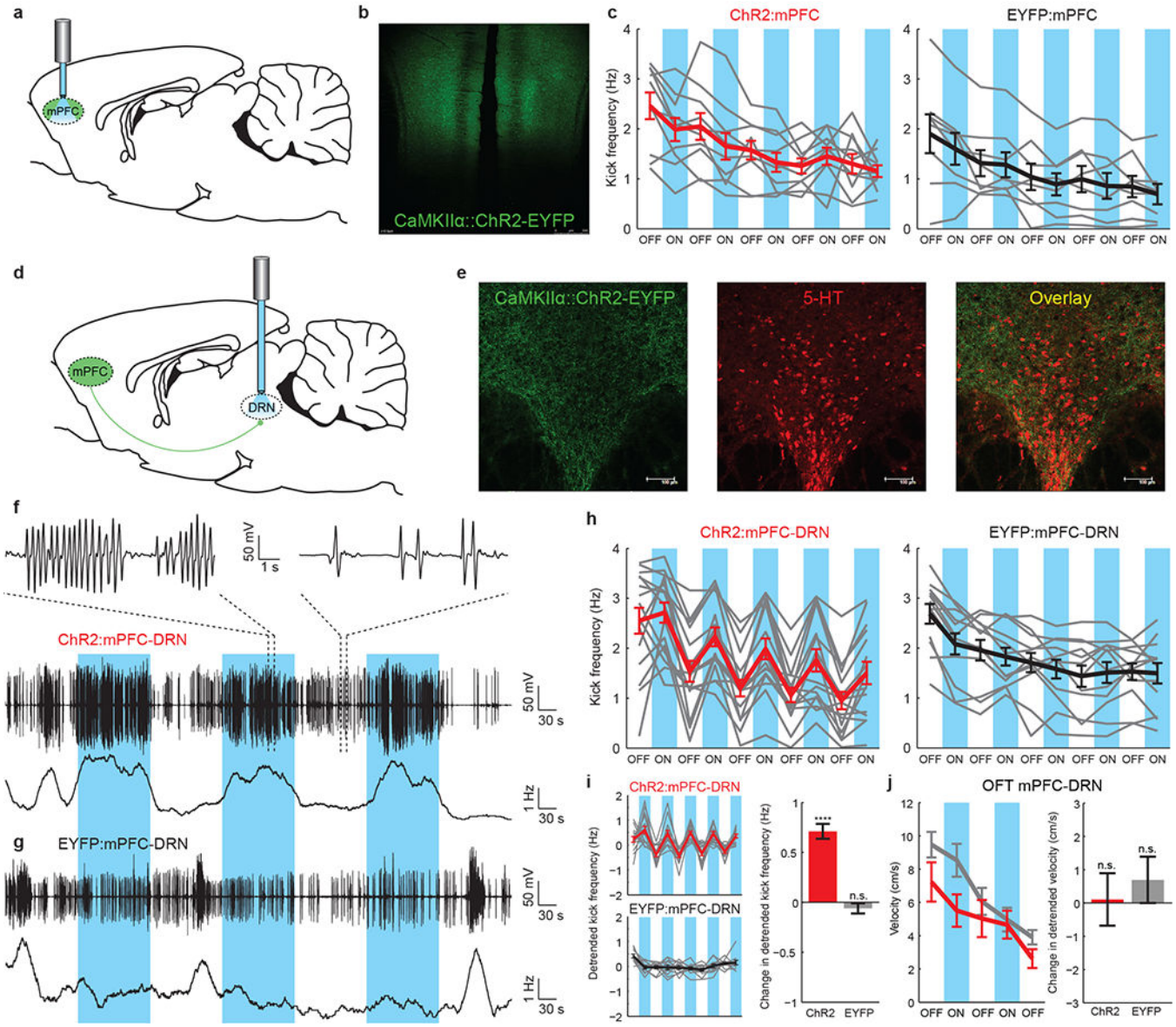

Figure 3. Optogenetic stimulation of mPFC axons in the DRN, but not excitatory mPFC cell bodies, induces behavioral activation

a) ChR2-EYFP or EYFP-expressing mPFC principal neurons were directly illuminated. **b)** ChR2-EYFP fluorescence in the mPFC. **c)** FST kick frequency for ChR2:mPFC (left, n=10) and EYFP:mPFC (right, n=8) rats. Gray lines: individual rats. Thick lines: average for ChR2:mPFC (red) or EYFP:mPFC (black) rats. Blue bars: light on. **d)** A fiber optic was implanted over the DRN after mPFC injection. **e)** ChR2-EYFP fluorescence in mPFC axons in the DRN (immunostained for 5-HT). **f)** FST behavioral data from one ChR2:mPFC-DRN rat. Top, middle: coil voltage. Bottom: kick frequency. **g)** FST data from one EYFP:mPFC-DRN rat. **h)** FST kick frequency for all rats. Left: ChR2:mPFC-DRN rats (n=16). Right: EYFP:mPFC-DRN rats (n=12). **i)** Left: exponentially detrended data from **h**. Right: change in detrended kick frequency from light-off to light-on epochs, ChR2:mPFC-DRN (red) and EYFP:mPFC-DRN (gray) rats. **j)** Left: velocity during stimulation in the open field test.

Red: ChR2:mPFC-DRN rats (n=12). Gray: EYFP:mPFC-DRN rats (n=12). Right: change in detrended velocity from light-off to light-on epochs. Error bars indicate s.e.m.

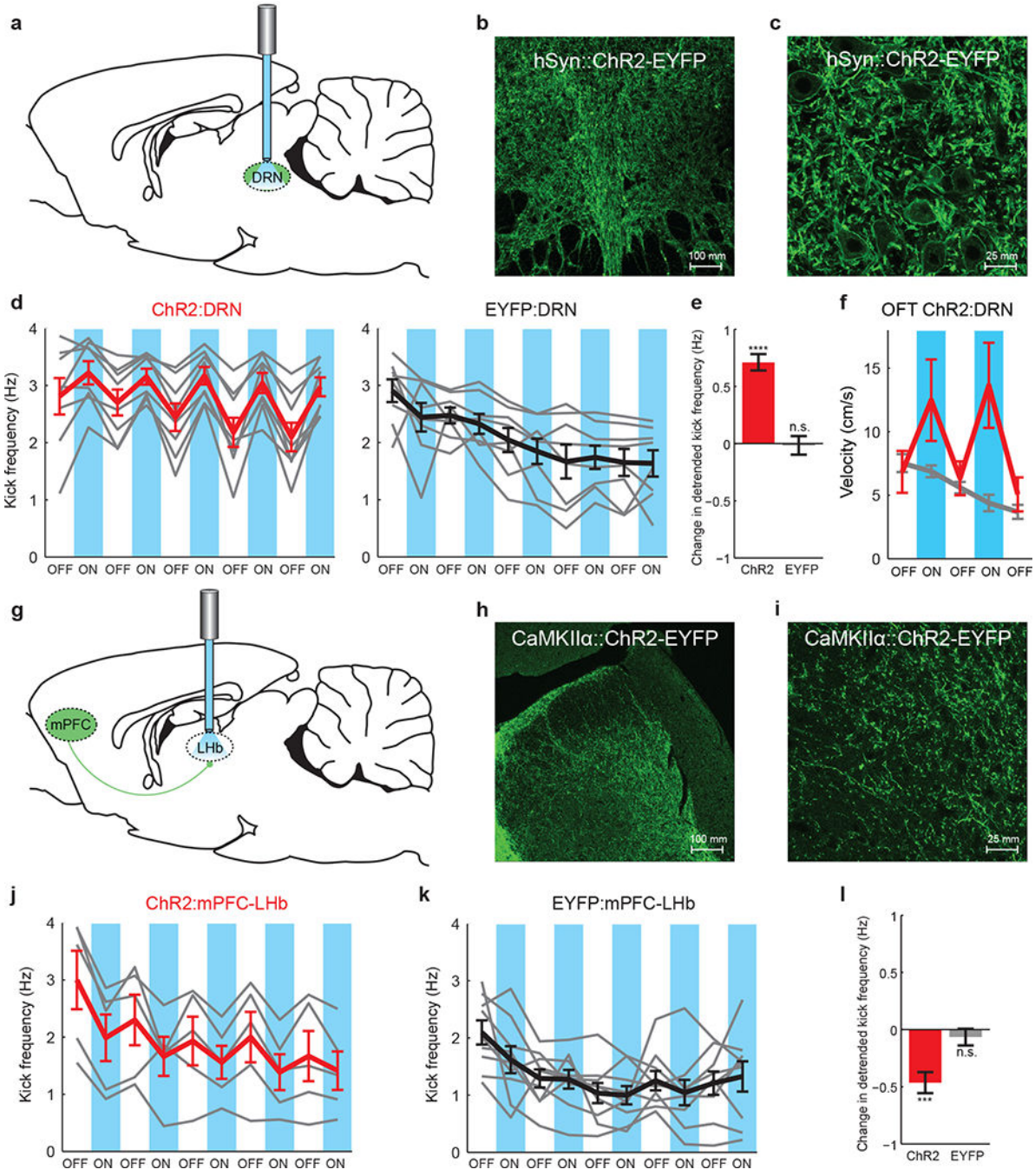

Figure 4. Behavioral activation resulting from stimulation of DRN-projecting mPFC axons is specific to the mPFC-DRN synapse

a) A fiber optic was implanted over ChR2- or EYFP-expressing neurons in the DRN. **b)** 20× image of ChR2-EYFP-expressing DRN neuronal cell bodies. **c)** 40×2× DRN image. **d)** FST kick frequency for all rats. Left: ChR2:DRN rats (n=8). Right: EYFP:DRN rats (n=8). Gray lines: individual rats. Thick lines: average for ChR2:DRN (red) or EYFP:DRN (black) rats. Blue bars: light on. **e)** Detrended change in kick frequency from light-off to light-on epochs, ChR2:DRN (red) and EYFP:DRN (gray) rats. **f)** Velocity during stimulation in the open field

test. Red: ChR2:DRN (n=12), Gray:EYFP:DRN (n=12) rats. **g)** Fiber optics were implanted bilaterally over the LHb to activate ChR2-expressing LHb-projecting mPFC axons. **h)** 20× image of ChR2-EYFP-expressing mPFC axons in the LHb. **i)** 40×2× LHb image. **j)** FST kick frequency for all rats. Left: ChR2:mPFC-LHb rats (n=5). Right:EYFP:mPFC-LHb rats (n=9). **k)** Detrended change in kick frequency from light-off to light-on epochs in the FST. Error bars indicate s.e.m.